

01 Sep 2011

Analysis and Finite Element Approximation of a Coupled, Continuum Pipe-Flow/Darcy Model for Flow in Porous Media with Embedded Conduits

Yanzhao Cao


Max Gunzburger

Fei Hua

Xiaoming Wang

Missouri University of Science and Technology, xiaomingwang@mst.edu

Follow this and additional works at: https://scholarsmine.mst.edu/math_stat_facwork

 Part of the [Mathematics Commons](#), and the [Statistics and Probability Commons](#)

Recommended Citation

Y. Cao et al., "Analysis and Finite Element Approximation of a Coupled, Continuum Pipe-Flow/Darcy Model for Flow in Porous Media with Embedded Conduits," *Numerical Methods for Partial Differential Equations*, vol. 27, no. 5, pp. 1242 - 1252, Wiley, Sep 2011.

The definitive version is available at <https://doi.org/10.1002/num.20579>

This Article - Journal is brought to you for free and open access by Scholars' Mine. It has been accepted for inclusion in Mathematics and Statistics Faculty Research & Creative Works by an authorized administrator of Scholars' Mine. This work is protected by U. S. Copyright Law. Unauthorized use including reproduction for redistribution requires the permission of the copyright holder. For more information, please contact scholarsmine@mst.edu.

Analysis and Finite Element Approximation of a Coupled, Continuum Pipe-Flow/Darcy Model for Flow in Porous Media with Embedded Conduits

Yanzhao Cao,¹ Max Gunzburger,² Fei Hua,³ Xiaoming Wang³

¹Department of Mathematics and Statistics, Auburn University, Auburn, Alabama 36830

²Department of Scientific Computing, Florida State University, Tallahassee, Florida 32306

³Department of Mathematics, Florida State University, Tallahassee, Florida 32306

Received 25 July 2009; accepted 14 October 2009

Published online 29 March 2010 in Wiley Online Library (wileyonlinelibrary.com).

DOI 10.1002/num.20579

We consider the continuum Darcy/pipe flow model for flows in a porous matrix containing embedded conduits; such coupled flows are present in, e.g., karst aquifers. The mathematical well-posedness of the coupled problem as well as convergence rates of finite element approximation are established in the two-dimensional case. Computational results are also provided. © 2010 Wiley Periodicals, Inc. *Numer Methods Partial Differential Eq* 27: 1242–1252, 2011

Keywords: finite element; pipe flow; porous media flow

I. INTRODUCTION

Conventionally, the purely hydraulic interaction between flow in a porous media (also called a fissured system in the geological community) and the free flow in a conduit network embedded in the porous media is simulated by employing three types of modeling approaches [1]. First, multiple sets of fractures may be coupled to each other to represent the different hydraulic properties of the porous media and the conduit system [2]. Alternatively, double-continuum or multicontinuum models have been applied wherein the cross flow between the two systems depends on the corresponding pressure differences via linear exchange terms [3–6]. As a third approach, discrete networks of flow paths can be coupled to a continuum model to model the dualistic flow patterns [7–9].

The last approach, the most used for geological studies, is referred to as the *coupled continuum pipe flow* (CCPF) model. As its name indicates, it is a coupled system consisting of a two- or three-dimensional continuum, the porous matrix, with an embedded one-dimensional conduit

Correspondence to: Fei Hua, Department of Mathematics, Florida State University, Tallahassee, Florida 32306 (e-mail: fhua@math.fsu.edu)

Contract grant sponsor: National Science Foundation; contract grant numbers: DMS0852491, DMS0620035

© 2010 Wiley Periodicals, Inc.

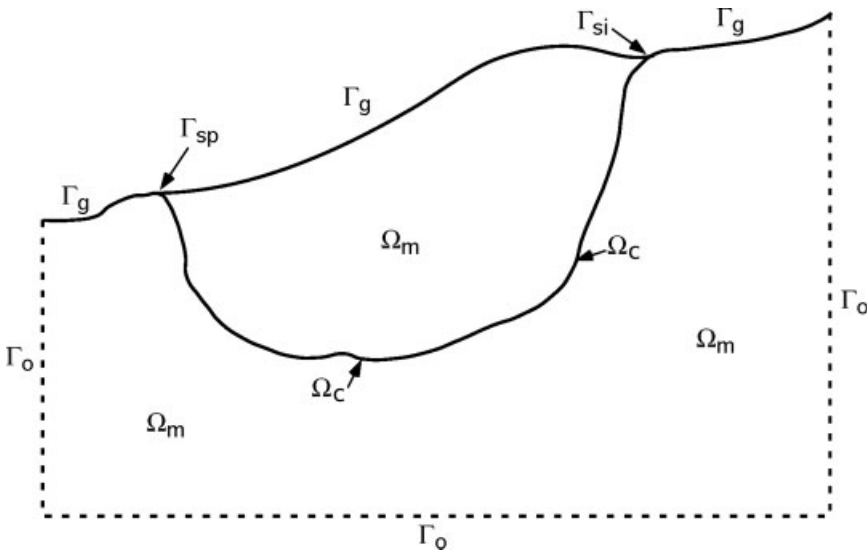


FIG. 1. Conceptual model of a karst aquifer having a conduit Ω_c embedded in a matrix Ω_m .

flow that is governed by the pipe flow model.¹ The flow in the matrix is governed by a Darcy-type system. It is used in [10–12] to study the genesis of karst aquifers and has achieved certain degree of success and acceptance.

A. The Coupled Pipe Flow/Darcy Model

We first review the formulation of the coupled pipe flow/Darcy model. Figure 1 provides a sketch of the conceptual model of a karst aquifer. In that figure, Ω_m and Ω_c denote the matrix and conduit domains, respectively, Γ_g the ground surface, Γ_{si} and Γ_{sp} a sinkhole and spring boundary, respectively, and Γ_o a bounding surface that is presumably far removed from the region of interest.

The flow in the porous matrix, Ω_m , is modeled by a continuum approach using the Boussinesq equation [13]

$$S \frac{\partial h_m}{\partial t} - \nabla \cdot (\mathbb{K} \nabla h_m) = \gamma, \tag{1.1}$$

where h_m denotes the hydraulic head in the porous matrix, \mathbb{K} the hydraulic conductivity tensor, S the storativity, and γ represents the volumetric rate of fluid transfer to the porous matrix system from the conduit system per unit length. We assume that $\mathbb{K} \in \mathbb{R}^{d \times d}$, $d = 2$ or 3 , is positive definite, i.e., there exist positive constants $c_1, c_2 > 0$ such that, for any $\mathbf{v} \in \mathbb{R}^d$,

$$c_1 \mathbf{v} \mathbf{v}^T \leq \mathbf{v} \mathbb{K} \mathbf{v}^T \leq c_2 \mathbf{v} \mathbf{v}^T.$$

For the conduit flow, the discharge can be related to the head difference in the tube by applying the Darcy-Weisbach equation [14]

¹Strictly speaking, for a two-dimensional problem, the fluid in the conduit is actually a channel flow. We refer to the conduit flow, no matter in two- or three-dimensional, as pipe flow for conciseness.

$$\frac{\partial h_c}{\partial \tau} = -\lambda \frac{u|u|}{2dg}, \tag{1.2}$$

where τ denotes the tangential direction along the one-dimensional pipe/channel conduit, d the pipe diameter (channel width for 2D),

$$u = \begin{cases} 4Q/(\pi d^2) & \text{for 3D} \\ Q/d & \text{for 2D} \end{cases},$$

the average velocity, g the gravitational acceleration, and Q the total discharge in the pipe. The friction factor, λ , depends on the velocity in the pipe via the Reynolds number $Re = |u|d/\nu$, with ν the kinematic viscosity of water. For low-flow velocities, laminar flow is assumed and the Hagen-Poiseuille equation can be applied. The friction factor for laminar flow is calculated as

$$\lambda = \begin{cases} \frac{64}{Re} = \frac{64\nu}{d|u|} & \text{for 3D} \\ \frac{24}{Re} = \frac{24\nu}{d|u|} & \text{for 2D.} \end{cases}$$

Substituting the above relation into (1.2), we have

$$Q = -D \frac{\partial h_c}{\partial \tau}, \quad \text{where } D = \begin{cases} \frac{\pi d^4 g}{128\nu} & \text{for 3D} \\ \frac{d^3 g}{12\nu} & \text{for 2D.} \end{cases}$$

Conservation of mass in the pipe implies that $\frac{\partial Q}{\partial \tau} = -\gamma$. Hence, we have

$$-\frac{\partial}{\partial \tau} \left(D \frac{\partial h_c}{\partial \tau} \right) = -\gamma. \tag{1.3}$$

The matrix and conduit flows are coupled at their intersection by the quasi-steady-state exchange term [3, 15]

$$\gamma = \alpha_{ex}(h_c - h_m), \tag{1.4}$$

where $\alpha_{ex} > 0$ is the exchange coefficient. This is equivalent to saying that the process in the conduit is enslaved by that in the porous matrix.

As a result, in the steady-state case, we have the system

$$\begin{cases} -\nabla(\mathbb{K}\nabla h_m) = -\alpha_{ex}(h_m - h_c)\delta_{\Omega_c} + f_m & \text{in } \Omega_m \\ -\frac{\partial}{\partial \tau} \left(D \frac{\partial h_c}{\partial \tau} \right) = \alpha_{ex}(h_m - h_c) + f_c & \text{in } \Omega_c, \end{cases} \tag{1.5}$$

where f_m and f_c denote the external source or sink, Ω_m and Ω_c denote the regions for the porous matrix and pipe conduit, respectively, and δ_{Ω_c} represents the Dirac δ function concentrated on Ω_c . (1.5) is essentially two coupled Poisson equations in different dimensions.

The time-dependent version of (1.5) first appeared in [10, 11, 16], where karst aquifer genesis is studied. The model was originally borrowed from dual-porosity models [3–6]. The finite element

discretization for the coupled nonlinear Richard’s equation and pipe (or plane) flow is discussed in [9, 17] for variably saturated porous media. However, no mathematical theory is available to guarantee existence of solutions and the coupling condition of the form (1.4) is not incorporated. Combining the idea of dual porosity and mimicking the numerical schemes in [9, 17], the model (1.5) in [10, 11, 16] is solved by the Carbonate Aquifer Void Evolution (CAVE) code [18]. CAVE solves the flow in the porous matrix by a finite difference scheme using MODFLOW [19] and the flow in conduit by a nonlinear finite difference discretization.² Then, the coupling exchange condition is reached by iteratively solving in the matrix and conduit regions. The exchange of fluid is only allowed at the discrete finite difference node points. No rigorous mathematical theory is presented therein to show well-posedness or guarantee convergence.

In this article, a systematic presentation of the analysis and numerical analysis of a simplified, *two-dimensional* problem is presented. The stationary case with fully saturated flow in the matrix and linear flow in the conduit is considered. The following geometrical setup is used. The matrix continuum is assumed to occupy the square $\Omega_m := (0, 1) \times (-1/2, 1/2) \subset \mathbb{R}^2$ and the one-dimensional conduit pipe lies in the middle $\Omega_c := I := (0, 1) \times \{0\}$. Then, (1.5) becomes

$$\begin{cases} -\nabla(\mathbb{K}\nabla h_m) = -\alpha_{ex}(h_m(x, 0) - h_c(x))\delta(y) + f_m & \text{in } \Omega_m \\ -\frac{d}{dx} \left(D \frac{dh_c}{dx} \right) = \alpha_{ex}(h_m|_{y=0} - h_c) + f_c & \text{in } \Omega_c, \end{cases} \tag{1.6}$$

where $\delta(y)$ denotes the Dirac delta function in y . In addition, we impose Dirichlet (fixed heads) boundary conditions

$$\begin{cases} h_m = g_m & \text{on } \partial\Omega_m \\ h_c = g_c & \text{on } \partial\Omega_c, \end{cases} \tag{1.7}$$

where g_m and g_c are given functions. We remark that we may also consider a three-dimensional porous matrix coupled with two-dimensional free-flow plane. The proof of well-posedness remains the same, whereas the regularity and numerical analysis can be treated in a very similar fashion. For the coupling of a three-dimensional porous matrix with a one-dimensional conduit, the rigorous mathematical treatment is not straightforward because the coupling introduces a forcing term to the Darcy equation governing the matrix having a strong singularity. Despite the lack of mathematical rigor, such three-dimensional/one-dimensional couplings are used, at the discrete level, in engineering practice.

II. WELL-POSEDNESS AND REGULARITY

In what follows, we only consider the homogeneous boundary case, i.e., we assume that $g_m \equiv 0$ and $g_c \equiv 0$. The nonhomogeneous case can be converted to the homogeneous case through the standard procedure of extending the boundary data to the whole domain and then considering the difference between the original unknown and the extension.

The variational formulation for the problem (1.6) can be derived in the usual manner by multiplying the equation by test functions and performing integration by parts. This leads to the bilinear form $a(\cdot, \cdot)$ on $\mathbf{H} \times \mathbf{H}$, where $\mathbf{H} := H_0^1(\Omega_m) \times H_0^1(\Omega_c)$, defined by

²The nonlinearity for the conduit only occurs for the turbulent case. Since we only consider laminar flow in the conduit, a nonlinear solver is not necessary.

$$\begin{aligned}
 a(\mathbf{h}, \mathbf{v}) &:= \int_{\Omega} \mathbb{K} \nabla h_m(x, y) \cdot \nabla v_m(x, y) dx dy + \int_0^1 D h'_c(x) v'_c(x) dx \\
 &+ \alpha_{\text{ex}} \int_0^1 (h_m(x, 0) - h_c(x)) v_m(x, 0) dx \\
 &- \alpha_{\text{ex}} \int_0^1 (h_m(x, 0) - h_c(x)) v_c(x) dx,
 \end{aligned} \tag{2.1}$$

where $\mathbf{h} = (h_m, h_c)$, $\mathbf{v} = (v_m, v_c) \in \mathbf{H}$.

We say that $\mathbf{h} \in \mathbf{H}$ is a weak solution of (1.6) if it satisfies

$$a(\mathbf{h}, \mathbf{v}) = (f_m, v_m)_{L^2(\Omega)} + (f_c, v_c)_{L^2(I)} \quad \forall \mathbf{v} \in \mathbf{H}. \tag{2.2}$$

Proposition 2.1. *Assume that $f_m \in H^{-1}(\Omega)$ and $f_c \in H^{-1}(I)$. Then, a weak solution \mathbf{h} of (1.6) exists, is unique, and satisfies the estimate*

$$\|\mathbf{h}\|_{\mathbf{H}} \leq C(\|f_m\|_{H^{-1}(\Omega)} + \|f_c\|_{H^{-1}(I)}), \tag{2.3}$$

where C is a constant independent of f_m and f_c .

Proof. The proof is a straightforward application of the Lax-Milgram theorem. We only need to verify the continuity and coercivity of the bilinear form $a(\cdot, \cdot)$ on $\mathbf{H} \times \mathbf{H}$.

The verification of the continuity is trivial and follows directly from the trace theorem since $\|h(\cdot, 0)\|_{L^2(I)} \leq C\|h\|_{H^1(\Omega)}$. The coercivity is also straightforward because, for $\mathbf{h} \in \mathbf{H}$, we have that

$$\begin{aligned}
 a(\mathbf{h}, \mathbf{h}) &= \int_{\Omega} \mathbb{K} \nabla h_m(x, y) \cdot \nabla h_m(x, y) dx dy + \int_0^1 D(h'_c(x))^2 dx \\
 &+ \alpha_{\text{ex}} \int_0^1 (h_m(x, 0) - h_c(x)) h_m(x, 0) dx \\
 &- \alpha_{\text{ex}} \int_0^1 (h_m(x, 0) - h_c(x)) h_c(x) dx \\
 &\geq \int_{\Omega} \mathbb{K} \nabla h_m(x, y) \cdot \nabla h_m(x, y) dx dy + \int_0^1 D(h'_c(x))^2 dx.
 \end{aligned} \quad \blacksquare$$

Next, we consider the regularity of the weak solution.

Proposition 2.2. *Let $\mathbf{h} = (h_m, h_c)$ denote the weak solution of (1.6). Assume that $f_m \in H^{-\frac{1}{2}}(\Omega)$ and $f_c \in L^2(I)$. Then, $\mathbf{h} \in H^{\frac{3}{2}-\epsilon}(\Omega) \times H^2(I)$ for all $\epsilon \in (0, \frac{1}{2})$ and*

$$\|\mathbf{h}\|_{H^{\frac{3}{2}-\epsilon}(\Omega) \times H^2(I)} \leq C(\epsilon) (\|f_m\|_{H^{-\frac{1}{2}}(\Omega)} + \|f_c\|_{L^2(I)}). \tag{2.4}$$

This regularity result is nearly optimal in the sense that there is no $\beta > 0$ such that $h_m \in H^{\frac{3}{2}+\beta}(\Omega)$, even if f_m and f_c are smooth.

Proof. The fact that $h_c \in H^2(I)$ is obvious. Indeed, by setting the test function v_m for the porous media identically to zero in the weak formulation (2.2), we see that h_c solves the one-dimensional elliptic problem

$$\int_0^1 (Dh'_c(x)v'_c(x) + \alpha_{ex}h_c(x)v_c(x))dx = \int_0^1 (\alpha_{ex}h_m(x, 0) + f_c(x))v_c(x)dx.$$

The regularity of h_c follows from classical elliptic regularity, the assumption that $f_c \in L^2(I)$, and the fact that $h_m(x, 0) \in H^{\frac{1}{2}}(I) \subset L^2(I)$.

As for the regularity of h_m , we notice that h_m solves the equation

$$\begin{aligned} \int_{\Omega} \mathbb{K} \nabla h_m(x, y) \cdot \nabla v_m(x, y) dx dy \\ = - \int_0^1 \alpha_{ex} (h_m(x, 0) - h_c(x)) v_m(x, 0) dx + \int_{\Omega} f_m v_m dx dy, \forall v_m \in H_0^1(\Omega). \end{aligned} \tag{2.5}$$

We further notice that, for $\epsilon \in (0, \frac{1}{2})$,

$$\begin{aligned} \int_0^1 (h_m(x, 0) - h_c(x)) v(x, 0) dx &\leq (\|h_m(\cdot, 0)\|_{L^2(I)} + \|h_c\|_{L^2(I)}) \|v(\cdot, 0)\|_{L^2(I)} \\ &\leq C(\epsilon) (\|h_m\|_{H^1(\Omega)} + \|h_c\|_{L^2(I)}) \|v\|_{H^{\frac{1}{2}+\epsilon}(\Omega)}. \end{aligned}$$

Therefore, $-\int_0^1 \alpha_{ex} (h_m(x, 0) - h_c(x)) v_m(x, 0) dx$ defines a bounded linear functional $\tilde{f}_m \in H^{-\frac{1}{2}-\epsilon}(\Omega)$ on $H_0^{\frac{1}{2}+\epsilon}(\Omega)$, and

$$\|\tilde{f}_m\|_{H^{-\frac{1}{2}-\epsilon}(\Omega)} \leq C(\epsilon) (\|f_m\|_{H^{-1}(\Omega)} + \|f_c\|_{H^{-1}(I)}).$$

Henceforth, thanks to classical elliptic regularity results for domains with corners [20], we have that $h_m \in H^{\frac{3}{2}-\epsilon}(\Omega)$ since the right-hand side of (2.5), $\tilde{f}_m + f_m$, belongs to $H^{-\frac{1}{2}-\epsilon}(\Omega)$. Interpolation inequalities [21] may be invoked, where necessary, for orders involving 1/2. Higher regularity of f_m or f_c does not improve the results.

As for the near optimal regularity, we notice that a simple calculation indicates that

$$\delta(y) \in H^{-\frac{1}{2}-\epsilon}(\Omega) \quad \forall \epsilon > 0,$$

but not any better (unless one resorts to anisotropic Sobolev spaces or non-Hilbert spaces). Now, if h_m were more regular and belonged to $H^{\frac{3}{2}+\beta}(\Omega)$ for some $\beta > 0$, it would imply that³

$$\delta(y)(h_m(x, y) - h_c(x)) \in H^{-\frac{1}{2}-\epsilon}(\Omega), \quad \forall \epsilon > 0.$$

This contradicts the first equation in (1.6) (which is valid in the distributional sense) since the regularity of the left-hand side would be $H^{-\frac{1}{2}+\beta}(\Omega)$ under the assumption that $h_m \in H^{\frac{3}{2}+\beta}(\Omega)$, and this is not consistent with the optimal regularity of the right-hand side ($H^{-\frac{1}{2}-\epsilon}(\Omega)$). ■

³This is true because, for any $f_1 \in H_0^{\frac{1}{2}+\epsilon}(\Omega)$, $\epsilon > 0$ and $f_2 \in H^{1+\beta}(\Omega)$, $\beta > 0$, their product, $f_1 f_2$, belongs to $H_0^{\frac{1}{2}+\epsilon}(\Omega)$ [20].

Remark 2.3. In the case of homogeneous isotropic matrix, i.e., $\mathbb{K} = k\mathbb{I}$, one can easily check via separation of variable that we have higher order piecewise regularity in the sense that $h_m|_{\Omega \cap \{y>0\}} \in H^{2+\epsilon}(\Omega \cap \{y > 0\})$, $h_m|_{\Omega \cap \{y<0\}} \in H^{2+\epsilon}(\Omega \cap \{y < 0\})$ for any $\epsilon \in (0, \frac{1}{2})$.

III. FINITE ELEMENT APPROXIMATIONS

In this section, we construct and analyze finite element approximations for the weak solution of (1.6). Let Ω_h denote a regular triangulation [22] of Ω and I_h be a regular partition of I . We construct the finite element subspaces $H_m^h \subset H_0^1(\Omega)$ and $H_c^h \subset H_0^1(I)$ consisting of continuous piecewise polynomials of order $k \geq 1$ with respect to Ω_h and I^h , respectively, where h denotes a measure of the mesh size. The finite element approximation $\mathbf{h}^h = (h_m^h, h_c^h) \in \mathbf{H}^h := H_m^h \times H_c^h$ of the weak solution \mathbf{h} of (1.6) is determined from

$$a(\mathbf{h}^h, \mathbf{v}^h) = (f_m, v_m^h)_{L^2(\Omega)} + (f_c, v_c^h)_{L^2(I)}, \quad \forall \mathbf{v}^h = (v_m^h, v_c^h) \in \mathbf{H}^h. \tag{3.1}$$

By the regularity result of Proposition 2.2 and a standard argument for finite element approximations, we have the following error estimate.

Theorem 3.1. (3.1) admits a unique solution $\mathbf{h}^h = (h_m^h, h_c^h) \in \mathbf{H}^h$. Moreover, for $0 < \epsilon < \frac{1}{2}$, there exists a constant $C(\epsilon)$ independent of h such that

$$\begin{aligned} \|\mathbf{h} - \mathbf{h}^h\|_{\mathbf{H}} &\leq C(\epsilon)h^{\frac{1}{2}-\epsilon} \\ \|\mathbf{h} - \mathbf{h}^h\|_{L^2(\Omega) \times L^2(I)} &\leq C(\epsilon)h^{1-2\epsilon}. \end{aligned} \tag{3.2}$$

Furthermore, if a given exact solution h_m is piecewise smooth in the sense that $h_m|_{y>0} \in H^{k+1}(\Omega \cap \{y > 0\})$, $h_m|_{y<0} \in H^{k+1}(\Omega \cap \{y < 0\})$, and $h_c \in H^{k+1}(I)$, and if the finite elements are chosen so that I does not intersect with the interior of any element from Ω_h , we have the following estimates with improved convergence rates:

$$\begin{aligned} \|\mathbf{h} - \mathbf{h}^h\|_{\mathbf{H}} &\leq Ch^k, \\ \|\mathbf{h} - \mathbf{h}^h\|_{L^2(\Omega) \times L^2(I)} &\leq C(\epsilon)h^{k+\frac{1}{2}-\epsilon}. \end{aligned} \tag{3.3}$$

Proof. The proof of the well-posedness of the finite element problem (3.1) is the same as that for the well-posedness of the PDE given in Proposition 2.1.

Recall that we have the well-known approximation inequalities

$$\begin{aligned} \|\mathbf{h} - \mathcal{I}_k^h(\mathbf{h})\|_{\mathbf{H}} &\leq Ch^l \|\mathbf{h}\|_{H^{l+1}(\Omega) \times H^{l+1}(I)} \\ \|\mathbf{h} - \mathcal{I}_k^h(\mathbf{h})\|_{\mathbf{H}} &\leq C \|\mathbf{h}\|_{\mathbf{H}} \end{aligned}$$

for all $0 \leq l \leq k$, where C is a constant with value independent of \mathbf{h} and h , and \mathcal{I}_k^h denotes the classical interpolation operator by continuous piecewise polynomials of order k ([22, Chapter 4]). Utilizing the interpolation theorem [23], we obtain

$$\|\mathbf{h} - \mathcal{I}_k^h(\mathbf{h})\|_{\mathbf{H}} \leq C(\epsilon)h^{\frac{1}{2}-\epsilon} \|\mathbf{h}\|_{H^{\frac{3}{2}-\epsilon}(\Omega) \times H^{\frac{3}{2}-\epsilon}(I)}, \forall k.$$

A standard finite element error estimates together with the continuity and coercivity of the bilinear form $a(\cdot, \cdot)$ on $\mathbf{H} \times \mathbf{H}$ leads to

$$\begin{aligned} \|\mathbf{h} - \mathbf{h}^h\|_{\mathbf{H}} &\leq C \inf_{\tilde{\mathbf{h}}^h \in \mathbf{H}^h} \|\mathbf{h} - \tilde{\mathbf{h}}^h\|_{\mathbf{H}} \\ &\leq C \|\mathbf{h} - \mathcal{I}_k^h(\mathbf{h})\|_{\mathbf{H}} \\ &\leq C(\epsilon)h^{\frac{1}{2}-\epsilon} \|\mathbf{h}\|_{H^{\frac{3}{2}-\epsilon}(\Omega) \times H^{\frac{3}{2}-\epsilon}(I)}. \end{aligned}$$

As for the L^2 error estimate in (3.2), we apply the classical Aubin-Nitsche technique to deduce that

$$\begin{aligned} \|\mathbf{h} - \mathbf{h}^h\|_{L^2(\Omega) \times L^2(I)}^2 &= a(\mathbf{h} - \mathbf{h}^h, \phi) \\ &= a(\mathbf{h} - \mathbf{h}^h, \phi - \psi^h) \quad \forall \psi^h \in \mathbf{H}^h \\ &\leq C \|\mathbf{h} - \mathbf{h}^h\|_{\mathbf{H}} \inf_{\psi^h \in \mathbf{H}^h} \|\phi - \psi^h\|_{\mathbf{H}} \\ &\leq C(\epsilon)h^{1-2\epsilon} \|\mathbf{h}\|_{H^{\frac{3}{2}-\epsilon}(\Omega) \times H^{\frac{3}{2}-\epsilon}(I)} \|\phi\|_{H^{\frac{3}{2}-\epsilon}(\Omega) \times H^{\frac{3}{2}-\epsilon}(I)} \\ &\leq C(\epsilon)h^{1-2\epsilon} \|\mathbf{h} - \mathbf{h}^h\|_{L^2(\Omega) \times L^2(I)}, \end{aligned}$$

where $\phi \in \mathbf{H}$ solves the adjoint problem

$$a(\mathbf{v}, \phi) = (\mathbf{h} - \mathbf{h}^h, \mathbf{v})_{L^2(\Omega) \times L^2(I)}, \quad \forall \mathbf{v} \in \mathbf{H},$$

and we have applied the regularity estimate (2.4).

If the exact solution \mathbf{h} is piecewise smooth as assumed, then we have the better estimates stated in (3.3). Indeed, in this case we have

$$\begin{aligned} \|\mathbf{h} - \mathbf{h}^h\|_{\mathbf{H}} &\leq C \inf_{\tilde{\mathbf{h}}^h \in \mathbf{H}^h} \|\mathbf{h} - \tilde{\mathbf{h}}^h\|_{\mathbf{H}} \leq C \|\mathbf{h} - \mathcal{I}_k^h(\mathbf{h})\|_{\mathbf{H}} \\ &\leq Ch^k (\|\mathbf{h}\|_{H^{k+1}(\Omega \cap \{y>0\}) \times H^{k+1}(I)} + \|\mathbf{h}\|_{H^{k+1}(\Omega \cap \{y<0\}) \times H^{k+1}(I)}), \end{aligned}$$

where in the last step we have used the assumption that I does not intersect with the interior of any element from Ω_h and hence h_m is smooth on each element so that the classical interpolation error can be applied.

We also have, by the Nitsche-Aubin technique,

$$\begin{aligned} \|\mathbf{h} - \mathbf{h}^h\|_{L^2(\Omega) \times L^2(I)}^2 &\leq C \|\mathbf{h} - \mathbf{h}^h\|_{\mathbf{H}} \inf_{\psi^h \in \mathbf{H}^h} \|\phi - \psi^h\|_{\mathbf{H}} \\ &\leq C(\epsilon)h^{k+\frac{1}{2}-\epsilon} \|\phi\|_{H^{\frac{3}{2}-\epsilon}(\Omega) \times H^{\frac{3}{2}-\epsilon}(I)} \\ &\leq C(\epsilon)h^{k+\frac{1}{2}-\epsilon} \|\mathbf{h} - \mathbf{h}^h\|_{L^2(\Omega) \times L^2(I)}. \end{aligned}$$

■

Remark 3.2. If we assume further regularity of solutions to the PDE (2.2) in the sense that, for all $H^{k-1}(\Omega_m)$ data, we have piecewise $H^{k+1}(\Omega \cap \{y > 0\})$ and $H^{k+1}(\Omega \cap \{y < 0\})$ solutions for h_m and

TABLE I. Convergence rate for steady-state problem with piecewise linear elements.

h	$\ h_c - h_c^h\ _0$	$\ h_m - h_m^h\ _0$	$ h_c - h_c^h _1$	$ h_m - h_m^h _1$
2^{-2}	$3.045E-1$	$1.648E-1$	3.867	2.250
2^{-3}	$7.959E-2$	$4.244E-2$	1.994	1.164
2^{-4}	$2.012E-2$	$1.069E-2$	1.005	$5.869E-1$
2^{-5}	$5.045E-3$	$2.677E-3$	$5.033E-1$	$2.941E-1$
2^{-6}	$1.262E-3$	$6.696E-4$	$2.518E-1$	$1.471E-1$
Rate of conv.*	1.981	1.987	0.987	0.985

*The convergence rate is obtained by fitting the the data in log–log scale by a straight line in the least-squares sense.

$$\begin{aligned} & \| \mathbf{h} \|_{H^{k+1}(\Omega \cap \{y>0\}) \times H^{k+1}(I)} + \| \mathbf{h} \|_{H^{k+1}(\Omega \cap \{y<0\}) \times H^{k+1}(I)} \\ & \leq C(\|f_m\|_{H^{k-1}(\Omega)} + \|f_c\|_{H^{k-1}(I)}), \end{aligned}$$

then we would obtain the optimal convergence rate $k + 1$ in L^2 for approximations with piecewise polynomials of order k . Such piecewise regularity holds for homogeneous isotropic matrix with $k = 1$ according to remark (2.3).

IV. COMPUTATIONAL RESULTS

We consider the two-dimensional setting. For convenience, we set all parameters in (1.5), including the hydraulic conductivity, to unity. We adjust the forcing functions f_m and f_c in Ω_m and Ω_c , respectively, so that the exact solution is given by

$$\begin{cases} h_c = 2 \sin(2\pi x) & \text{in } \Omega_c \\ h_m = \sin(2\pi x) & \text{in } (0, 1) \times (-1/2, 0] \subset \Omega_m \\ h_m = \left(-\frac{\alpha_{\text{ex}}}{\mathbb{K}} y + 1\right) \sin(2\pi x) & \text{in } (0, 1) \times [0, 1/2) \subset \Omega_m. \end{cases} \quad (4.1)$$

We use the piecewise linear or piecewise quadratic finite element spaces, i.e., $k = 1$ or 2 , respectively, based on uniform grids. The computational errors obtained and the estimated convergence rates are summarized in Tables I and II.

The second-order convergence rate for the L^2 norm of the error and the first-order convergence rate for the H^1 norm for piecewise linear elements completely agrees with our analysis since we are dealing with homogeneous isotropic matrix in this numerical example and hence we have piecewise regularity; see remarks (2.3 and 3.2).

The second order convergence rate in the H^1 norm agrees with our theoretical prediction with $k = 2$ since the chosen exact solution is piecewise smooth in the upper and lower regions and I

TABLE II. Convergence rate for steady-state problem with piecewise quadratic elements.

h	$\ h_c - h_c^h\ _0$	$\ h_m - h_m^h\ _0$	$ h_c - h_c^h _1$	$ h_m - h_m^h _1$
2^{-2}	$3.047E-2$	$1.644E-2$	$7.888E-1$	$6.906E-2$
2^{-3}	$3.907E-3$	$2.092E-3$	$2.025E-1$	$1.517E-2$
2^{-4}	$4.915E-4$	$2.628E-4$	$5.096E-2$	$3.582E-3$
2^{-5}	$6.153E-5$	$3.290E-5$	$1.276E-2$	$8.818E-4$
2^{-6}	$7.694E-6$	$4.114E-6$	$3.191E-3$	$2.198E-4$
Rate of conv.	2.989	2.992	1.987	2.070

does not intersect with the interior of any element from Ω_h . The better-than-predicted convergence rate in the L^2 norm may be explained via Remark 3.2, although it is not known if the piecewise regularity assumed in that remark for the solution of (2.2) is true in general.

V. CONCLUDING REMARKS

In this article, we addressed several mathematical issues regarding the CCFP model that is of increasing interest in the geological science community. A weak formulation of the linear stationary CCFP model is presented and its well-posedness is demonstrated. Finite element discretizations are then constructed and analyzed. Optimal convergence rates in the L^2 and H^1 norms are derived for the piecewise linear element case, and an optimal H^1 convergence rate for piecewise quadratic elements is derived under the assumption that the exact solution is piecewise smooth. However, we obtain better-than-expected numerical convergence rate in the L^2 norm. This is a likely consequence of the proper alignment of the grids and possible piecewise higher regularity of the solution for generic forcing.

Comparisons of results obtained using the coupled continuum/pipe flow model to the coupled Stokes-Darcy system with Beavers-Joseph or the simplified Beavers-Joseph-Saffman interface boundary condition (see [24–28]) are underway. The investigation of the three-dimensional problem is also underway. As they stand, the analyses presented in this article, do not hold for the three-dimensional case due to the stronger (compared with the two-dimensional case) singular nature of the line Dirac delta function in three dimensions.

This work is part of the Ph.D. thesis of Fei Hua written under the supervision of the second and the fourth authors. The authors thank Bill Hu who introduced them to the pipe flow model.

References

1. G. Teutsch and M. Sauter, Distributed parameter modeling approaches in karst-hydrological investigations, *Bull Hydrogéol* 16 (1998), 99–109.
2. W. Dershovitz, P. Wallmann, and S. Kindred, Discrete fracture network modeling for the Stripa site characterization and validation drift inflow predictions, SKB Stripa technical report TR-91-16, Swed Nucl Power and Waste Manage Co, Stockholm, 1991.
3. G. I. Barenblatt, I. P. Zheltov, and I. N. Kochina, Basic concepts in the theory of seepage of homogeneous liquids in fissured rocks, *J Appl Math Meth (USSR)* 24 (1960), 1286–1303.
4. Y. Cao, H. Wang, and X. Xie, Dual-media flow models of karst areas and their application in north China, In *Karst hydrogeology and karst environment protection: 21st Congress of the International Association of Hydrogeologists*, Guilin, China, International Association of Hydrogeol, 1988.
5. M. Sauter, Quantification and forecasting of regional groundwater flow and transport in a karst aquifer, Gallusquelle, Malm SW Germany, University of Tübingen, Germany, 1992, p. 150.
6. G. Teutsch, Two practical examples from the Swabian Alb, S Germany, In *4th Conference on Solving Groundwater Problems with Models*, Indianapolis, Int Ground Water Model Cent, 1989.
7. Y. Chen and J. Bian, The media and movement of karst water, In *karst hydrogeology and karst environment protection: 21st Congress of the International Association of Hydrogeologists*, Guilin, China, International Association of Hydrogeol, 1988.
8. L. Kiraly, Régularisation de l'areuse (Jura Suisse) simulée par modèle mathématique, *Hydrology of karstic terraines*, Verlag Heinz Heise, Hannover, Germany, 1984, pp. 94–99.
9. K. T. B. MacQuarrie and E. A. Sudicky, On the incorporation of drains into three-dimensional variably saturated groundwater flow models, *Water Resour Res* 32 (1996), 447–482.

10. S. Bauer, R. Liedl, and M. Sauter, Modeling of karst aquifer genesis: influence of exchange flow, *Water Resour Res* 39 (2003), SBH6.1–SBH6.12.
11. S. Birk, R. Liedl, M. Sauter, and G. Teutsch, Hydraulic boundary conditions as a controlling factor in karst genesis, *Water Resour Res* 39 (2003), SBH2.1–SBH2.14.
12. R. Liedl, M. Sauter, D. Hückinghaus, T. Clemens, and G. Teutsch, Simulation of the development of karst aquifers using a coupled continuum pipe flow model, *Water Resour Res* 39 (2003), SBH6.1–SBH6.11.
13. J. Bear and A. Verruijt, *Modeling groundwater flow and pollution*, D. Reidel Pub Co, Norwell, MA, 1987.
14. E. Bobok, *Fluid mechanics for petroleum engineers*, Elsevier Sci, New York, 1993.
15. T. N. Narasimhan, Multidimensional numerical simulation of fluid flow in fractured porous media, *Water Resour Res* 18 (1982), 1235–1247.
16. S. Bauer, R. Liedl, and M. Sauter, Modelling of karst development considering conduit-matrix exchange flow, Calibration and reliability in groundwater modelling: coping with uncertainty, *IAHS Publ* 265 (2000), 10–15.
17. R. Therrien and E. A. Sudicky, Three-dimensional analysis of variably-saturated flow and solute transport in discretely-fractured porous media, *J Contam Hydrol* 23 (1995), 1–44.
18. T. Clemens, D. Hückinghaus, M. Sauter, R. Liedl, and G. Teutsch, A combined continuum and discrete network reactive transport model for the simulation of karst development, *IAHS Publ* 237 (1996), 309–318.
19. A. Harbaugh, Modflow-2005, the U.S. Geological survey modular ground-water model—the Ground-Water Flow Process, U.S. Geological Survey Techniques and Methods 6-A16 (2005).
20. P. Grisvard, *Elliptic problems in nonsmooth domains*, Vol. 24, Longman Higher Education, London, UK, 1986.
21. R. A. Adams and J. J. Fournier, *Sobolev spaces*, Academic Press, Oxford, UK, 2003.
22. S. C. Brenner and L. R. Scott, *The mathematical theory of finite element methods*, Springer, New York, 2007.
23. J. Lions and E. Magenes, *Problèmes aux limites nonhomogènes et applications*, Vol. 1, Dunod, Paris, France.
24. Y. Cao, M. Gunzburger, X. Hu, F. Hua, X. Wang, and W. Zhao, Finite element approximation for time-dependent Stokes-Darcy flow with Beavers-Joseph interface boundary condition, *SIAM J Numer Anal* 47 (2010), 4239–4256.
25. Y. Cao, M. Gunzburger, F. Hua, and X. Wang, Coupled Stokes-Darcy model with Beavers-Joseph interface boundary condition, *Comm Math Sci* 8 (2010), 1–25.
26. M. Discacciati, E. Miglio, and A. Quarteroni, Mathematical and numerical models for coupling surface and groundwater flows, *Appl Num Math* 43 (2002), 57–74.
27. M. Discacciati and A. Quarteroni, Convergence analysis of a subdomain iterative method for the finite element approximation of the coupling of Stokes and Darcy equations, *Comput Vis Sci* 6 (2004), 93–103.
28. M. Mu and J. Xu, A two-grid method of a mixed Stokes-Darcy model for coupling fluid flow with porous media flow, *SIAM J Numer Anal* 45 (2007), 1801–1813.